Multi-view Latent Subspace Clustering based on both Global and Local Structure

Honghan Zhou HHANZHOU@OUTLOOK.COM
Weiling Cai CAIWL@NJNU.EDU.CN
Le Xu NJNUMASTERXU91@163.COM
Ming Yang MYANG@NJNU.EDU.CN
School of Computer and Electronic Information Nanjing Normal University Nanjing, China

Editors: Vineeth N Balasubramanian and Ivor Tsang

Abstract

Most existing multi-view clustering methods focus on the global structure or local structure among samples, and few methods focus on the two structures at the same time. In this paper, we propose a Multi-view Latent subspace Clustering based on both Global and Local structure (MLCGL). In this method, a latent embedding representation is learned by exploring the complementary information from different views. In the latent space, not only the global reconstruction relationship but also the local geometric structure among the latent variables are discovered. In this way, a unified affinity graph matrix is constructed in the latent space for different views, which indicates a clear between-class relationship. Meanwhile, a rank constraint is introduced on the Laplacian graph to facilitate the division of samples into the required clusters. In MLCGL, the affinity graph also provides positive feedback to optimize the learned latent representation and contribute to divided it into reasonable clusters. Moreover, we present an alternating iterative optimization scheme to optimize objective functions. Compared with the state-of-art algorithms, MLCGL has achieved excellent experimental performance on several real-world datasets.

Keywords: multi-view, latent represent, global and local structure, rank constraint

1. Introduction

With the continuous development of science and technology, the same data is usually comprised of several different views (Kang et al. (2020); Huang et al. (2020); Lin et al. (2021)). This is referred to as multi-view data, where each individual view constitutes a given task but each view also has its biases. The multi-view learning technology aims to integrate complementary information from different views to reduce the complexity of given task. And how to effectively use multi-view data has become a critical challenge faced by researchers.

Clustering which assigns the data into different groups with similarity, is a fundamental and important topic in machine learning. For multi-view scenarios, the traditional clustering algorithms usually process the view separately and choose the best result, or connect the features of all views as single-view data. But these algorithms fail to utilize the complementary information of different views and may cause excessively high dimensions of the data to be processed. To solve these problems, Kumar et al. (2011) introduced spectral clustering into multiple views application, which co-regularized the clustering indicator to achieve the same cluster membership on different views. And Peng and Cai (2021) captured the com-

patible intrinsic information across different views through low-rank sparse representation. Besides, (Xia et al. (2014); Zong et al. (2018); Nie et al. (2018)) explored the complementarity between views from the three aspects of Markov Chain, Spectral Perturbation, and Procrustes Analysis, which enhanced the finally clustering performance.

How to explore the similarity relationships among samples is also a research hotspot in multi-view clustering. In recent years, Huang et al. (2015) has pointed out that the similarity among samples can be represented in the form of global relationship or local relationship. The global relationship can be obtained by various manners, such as calculating the distance between every two samples Liu et al. (2013), computing the self-representation coefficient on training samples Ren and Sun (2020). The local relationship can be obtained by computing k-nearest neighbors, the local geometric structure, and so on. Some subspace clustering algorithms like Brbić and Kopriva (2018) perform the clustering by exploiting the global similarity among samples, it constructs the self-representation coefficient matrix of each view to indicate the global structure, and then introduces a regularization term to balance the global structure discrepancy between views. By contrast, the graph-based clustering algorithms (Nie et al. (2017); Wang et al. (2019)) usually utilize the local structure to build the affinity graphs and then perform clustering. They integrate the complementary information to build the shared graph, as a result, the clustering performance largely depends on the quality of the graph.

These multi-view clustering algorithms mentioned above mostly perform learning in the original space, but the original space usually has higher dimensions. To avoid this problem, Wang et al. (2020) project the multi-view data into a common subspace, then learn the common similarity graph from the local structure in the subspace. But, when the original space data is projected into the subspace, the noise will also be projected inevitably. To resist the influence of noise, Zhang et al. (2018) assumes that different views are all originated from one underlying latent representation, and then through the self-representation, the graph is learned to reflect the global structure of latent representation. Inspired by Zhang et al. (2018), Chen et al. (2020) introduced rank constraints on the Laplacian graph to implement the assignment of the sample points into designated clusters. However, (Zhang et al. (2018); Chen et al. (2020)) did not consider the local neighbor relationship in the latent space. Besides, (Huang et al. (2019a,b)) uses kernel tricks and neural network to learning nonlinear relationships.

In summary, in most existing multi-view clustering algorithms, few methods simultaneously mine the local and global similarity of data while avoiding the curse of dimensionality. To solve this issue, this paper proposes a novel algorithm named Multi-view Latent subspace Clustering based on both Global and Local structure (MLCGL). In MLCGL, a common latent representation is learned to capture the complementary information from different views. In the latent space, the global self-representation and local neighbor relationships are combined to construct a common affinity graph. In this way, the obtained affinity graph can more clearly reflect the within-class and the between-class relation. Based on this, a rank constraint is introduced on the Laplacian graph to group the data points in the latent space into a specified number of clusters. **The main contributions of this paper are: (1)** By learning the global and local structural relationships on the latent representation, the within-class and between-class relation in the affinity graph will be clarified, which promote the latent representation to be divided into more reasonable clusters. **2)** The common

latent representation which fuses the complementary information can suppress the possible noise while avoiding the curse of dimensionality. **3)** An iterative optimization scheme is presented to solve our proposed model. According to the experimental results, our algorithm can achieve the objective function convergence in a few iterations.

2. Related Work

2.1. Latent Multi-view Subspace Clustering (LMSC)

In LMSC Zhang et al. (2018), it is assumed that the multi-view data X^v is converted from a shared latent representation Y, that is $X^v = W^v Y + E_y^v, where E_y^v$ is the reconstruction error, and W^v is the transform matrix. Then, LMSC reconstructs the latent representation via self-representation: $Y = YZ + E_r$. Besides, LMSC introduced kernel norm constraint coefficient matrix Z to capture the global structure of the latent representation. Therefore, the overall objective function is:

$$\begin{aligned} &\min_{W,Y,Z,E_y,E_r} ||E_y||_{2,1} + \lambda_1 ||E_r||_{2,1} + \lambda_2 ||Z||_* \\ &s.t. X = WY + E_y, Y = YZ + E_r, WW^T = I \end{aligned} \tag{1}$$

where $X = [(X^1)^T, \cdots, (X^V)^T]^T, W = [(W^1)^T, \cdots, (W^V)^T]^T, and E_y = [(E_y^1)^T, \cdots, (E_y^V)^T]^T$ is the latent representation reconstruction error. λ_1, λ_2 are the hyper-parameters which are used to balance the different parts of the objective function. $||\cdot||_{2,1}, ||\cdot||_*$ denote $l_{2,1}$norm and nuclear norm, respectively.

2.2. Multi-view Clustering and Semi-supervised Classification with Adaptive Neighbours (MLAN)

Since high-dimensional data contains low-dimensional manifold structure Nie et al. (2016), MLAN Nie et al. (2017) introduces adaptive local structure to learn the inter-sample relationship for single view:

$$\min_{s_i} \sum_{i,j}^{n} ||x_i - x_j||_2^2 s_{ij} + \alpha ||S||_F^2 \quad s.t. \forall i, s_i^T 1 = 1, 0 \le s_{ij} \le 1 \tag{2}$$

where s_i is a vector with j-th element as $s_{i,j}$ in similarity matrix S. The regular term $||S||_F^2$ used to obtain an effective solution where $||\cdot||_2$ and $||\cdot||_F$ denote l_2-norm and the Frobenius norm respectively. And α is a hyper-parameter to balance the two terms. In addition, MLAN promotes the division of sample points into reasonable clusters by introducing rank constraints on the Laplacian graph L_s. Besides, MLAN believes that the quality of each view in the original space is different. Therefore, the objective function in MLAN can be formulated as:

$$\begin{aligned} &\min_{s_i} \sum_v (w_v \sum_{i,j}^{n} ||x_i^v - x_j^v||_2^2 s_{ij} + \gamma ||w_v||_2^2) + \alpha ||S||_F^2 \\ &s.t. \forall i, s_i^T 1 = 1, 0 \le s_{ij} \le 1, w_v^T 1 = 1, 0 \le w_v \le 1, rank(L_S) = n - c \end{aligned} \tag{3}$$

where $L_s = D - ((S^T + S))/2, D_{ij} = \sum_j (s_{ij} + s_{ji})/2$. Also, MLAN uses an optimization trick to turn the view weight into an adaptive parameter, and the final objective function is:

$$\begin{aligned} &\min_{s_i} \sum_v w_v \sum_{i,j}^{n} ||x_i^v - x_j^v||_2^2 s_{ij} + \alpha ||S||_F^2 \\ &s.t. \forall i, s_i^T 1 = 1, 0 \le s_{ij} \le 1, rank(L_S) = n - c \end{aligned} \tag{4}$$

where $w_v = 1/\sqrt{\sum_{i,j} ||x_i^v - x_j^v||_2^2 s_{ij}}$.

3. Proposed

Denote $\{X^1, \cdots, X^V\} \in \mathbb{R}^{d_v \times n}$ as multi-view data containing V views, each view has n samples, and d_v is the feature dimension of the v-th view. Denote $\{W^1, \cdots, W^V\}$as the corresponding transform matrices, and $Y = \{y_i\}_{i=1}^n$ as the shared latent representation. And $Tr(\cdot)$ denote the trace of the matrix.

3.1. Latent Representation

We represent multi-view data by different mappings of the latent representation: $X^v = W^v Y + E^v$, which E^v is the reconstruction error. In this way, the intrinsic relation between-views can be explored, and meanwhile the dimensionality of multi-view data can also be reduced. Besides, the possible noise may also be suppressed White et al. (2012). By minimizing the reconstruction error, the latent representation Y is encouraged to fully represent multi-view data, namely:

$$\min_{W^v} \sum_{v=1}^{V} ||X^v - W^v Y||_F^2 \quad s.t. W^{vT} W^v = I \tag{5}$$

3.2. Local and Global Structure Learning

Generally, most graph-based and subspace-based clustering algorithms only learn the similarity relationship separately from the local structure or the global structure, where cause the learned similarity relationship cannot fully indicate the relationship between samples. To this end, this paper will learn both local and global structure on the latent representation simultaneously to obtain a more comprehensive and robust affinity graph.

To mine the local structure hidden in the latent space, our model constructs the objective function as (6), meaning that the larger the Euclidean distance $||y_i - y_j||_2^2$ between two points, the smaller the corresponding probability s_{ij}:

$$\min_S \sum_{i,j} ||y_i - y_j||_2^2 s_{ij} \quad s.t. 1^T s_i = 1, s_{ij} > 0 \tag{6}$$

where S indicates the local similarity between samples, s_i is the column vector of S, and s_{ij} is the j-th element of s_i.

To further discover the global construction relationship in the latent space, our model adopts the self-representation and assumes that $Y = YZ + E_Y$. By minimizing the Frobenius norm of the reconstruction error E_Y, the reconstruction coefficient matrix Z can capture the global structure for the latent representation:

$$\min_{Z} ||Y - YZ||_F^2 \quad s.t. 1^T z_i = 1, z_{ij} > 0 \tag{7}$$

where Z indicates the global similarity between samples, z_i is the column vector of Z, and z_{ij} is the j-th element of z_i.

Therefore, we formulate the objective function (8) to learn the local and the global structure on the latent representation:

$$\min_{S} \sum_{i,j} ||y_i - y_j||_2^2 s_{ij} + ||Y - YS||_F^2 \quad s.t. 1^T s_i = 1, s_{ij} > 0 \tag{8}$$

In the iterative optimization process, the learned affinity graph will also contribute the latent representation to be divided into more reasonable clusters. The constructed graph considers the strengthens of the global structure and the local structure simultaneously, which achieves a balance of the two structure attributes. From the perspective of granularity, the structural information embodied by S tends to be cluster granularity. In this way, the unified graph induced by the similarity has a fuller diagonal block structure, which is also verified by the experimental results section. In this paper, the learned graph S reflects clearer distribution information between classes, so it is more conducive to subsequent clustering.

3.3. Rank Constraint

Ideally, the number of connected components in S is equal to the cluster number. But in fact, (8) usually cannot achieve this goal. In order to facilitate the learned affinity graph to be divided into connected components of a specified number, according to Theorem 1 Mohar et al. (1991), a rank constraint is introduced on the Laplacian graph L_S. That is, if rank $rank(L_S) = n - c$ holds, the corresponding graph S consists of c connected components.

Theorem 1

The multiplicity c of the eigenvalue 0 of the Laplacian matrix L_S of S is equal to the number of connected components in the graph with similarity matrix S.

Therefore, by introducing rank constraint, equation (8) is reformulated as:

$$\min_{S} \sum_{i,j} ||y_i - y_j||_2^2 s_{ij} + ||Y - YS||_F^2 \quad s.t. 1^T s_i = 1, s_{ij} > 0, rank(L_S) = n - c \tag{9}$$

3.4. Full Objective Function

Combining the aforementioned insights into analysis, we write the objective function of MLCGL as:

$$\begin{aligned} &\min_{W^v,Y,S,F} \sum_{v=1}^{V} ||X^v - W^v Y||_F^2 + \alpha \sum_{i,j} ||y_i - y_j||_2^2 s_{ij} + \beta ||Y - YS||_F^2 \\ &s.t. 1^T s_i = 1, s_{ij} > 0, W^{vT} W^v = I, rank(L_S) = n - c \end{aligned} \tag{10}$$

where α and β are the hyper-parameters used to control the weight of the local structure term and the global structure term, respectively. Because of the rank constraint, it is difficult for us to solve the objective function (10). Define σ_i as the i-th smallest eigenvalue on L_S, since Laplace matrix L_S is a positive semi-definite matrix, namely $\sigma_i > 0$, $rank(L_S) = n - c$ is equivalent to $\sum_{i=1}^{c} \sigma_i = 0$. According to Ky Fan's theorem Fan (1949):

$$\sum_{i=1}^{c} \sigma_i(L_S) = \min_{F^T F = I} Tr(F^T L_S F) \tag{11}$$

where F is the low-dimensional embedding matrix.

Thus the final objective function of MLCGL can be formulated as:

$$\begin{aligned} &\min_{W^v, Y, S, F} \sum_{v=1}^{V} ||X^v - W^v Y||_F^2 + \alpha \sum_{i,j} ||y_i - y_j||_2^2 s_{ij} \\ &+ \beta ||Y - YS||_F^2 + \gamma Tr(F^T L_S F) \\ &s.t. 1^T s_i = 1, s_{ij} > 0, W^{vT} W^v = I, F^T F = I \end{aligned} \tag{12}$$

where γ is used as a hyper-parameter to balance the proportion of rank constraints. When γ is large enough, the optimization objective function (12) will make $rank(L_s) = n - c$ hold.

3.5. Optimization

To address the objective function (12), we introduce an alternating optimization scheme to solve this problem.

Update F

When W^v, Y and S are all fixed, the problem of objective function (12) is equivalent to the following:

$$\min_{F} Tr(F^T L_S F) \quad s.t. F^T F = I \tag{13}$$

The optimal solution F can be obtained by c eigenvectors of L_S corresponding to the c smallest eigenvalues.

Update W

When the other variables are fixed, the problem of objective function (12) is equivalent to the following:

$$\min_{W^v} \sum_{v=1}^{V} ||X^v - W^v Y||_F^2 \quad s.t. W^{vT} W^v = I \tag{14}$$

Let $X = [(X^1)^T, \cdots, (X^V)^T]^T, W = [(W^1)^T, \cdots, (W^V)^T]^T$, then (14) can be rewritten as:

$$\min_{W} ||X - WY||_F^2 \quad s.t. W^T W = I \tag{15}$$

Since $||A||_F = ||A^T||_F$, so (15) is equivalent to:

$$\min_{W} ||X^T - Y^T W^T||_F^2 \quad s.t. W^T W = I \tag{16}$$

According to Theorem 2 Wahba (1965), the constraint condition needs to be $R^TR = RR^T = I$, but in Zhang et al. (2018), it is mentioned that relaxing the constraint to $R^TR = I$ can also obtain an optimal solution. From this, we can solve W by Theorem 2.

Theorem 2

Given the objective function $\min_R ||Q-GR||_F^2, s.t. R^TR = RR^T = I$, *the optimal solution is* $R = UV^T$, *where* U *and* V *are left and right singular values of SVD decomposition of* G^TQ.

Update Y

When the other variables are fixed, the problem of objective function (12) is equivalent to the following:

$$\min_Y \sum_{v=1}^{V} ||X^v - W^vY||_F^2 + \alpha \sum_{i,j} ||y_i - y_j||_2^2 s_{ij} + \beta ||Y - YS||_F^2 \tag{17}$$

And $\sum_{i,j} ||y_i - y_j||_2^2 s_{ij} = Tr(YL_SY^T)$, so (17) can be rewritten as:

$$\min_Y ||X - WY||_F^2 + \alpha Tr(YL_SY^T) + \beta ||Y - YS||_F^2 \tag{18}$$

Take the derivative with respect to Y and set it to zero:

$$W^TWY - W^TX + \alpha Y(L_S + L_S^T) + \beta(Y(I-S)(I-S)^T) = 0 \tag{19}$$

Because of $L_S = L_S^T$, Equation (19) is rewritten as:

$$W^TWY + Y \times (2\alpha L_S + \beta(I-S)(I-S)^T) = W^TX \tag{20}$$

Equation (20) is a standard Sylvester equation which has a unique solution by the Bartels-Stewart algorithm and there has a similar solution in Hu et al. (2014) or solved by MATLAB toolkit.

Update S

When the other variables are fixed, the problem of objective function (12) is equivalent to the following:

$$\begin{aligned} &\min_S \alpha \sum_{i,j} ||y_i - y_j||_2^2 s_{ij} + \beta ||Y - YS||_F^2 + \gamma Tr(F^TL_SF) \\ &s.t. 1^Ts_i = 1, s_{ij} > 0 \end{aligned} \tag{21}$$

Equation (21) is rewritten as:

$$\begin{aligned} &\min_S \alpha Tr(YL_SY^T) + \beta Tr(K - 2KS + S^TKS) + \gamma Tr(F^TL_SF) \\ &s.t. 1^Ts_i = 1, s_{ij} > 0 \end{aligned} \tag{22}$$

where $K = Y^TY$, and (22) can be rewritten in a column-wise manner as:

$$\min_{S_{:,i}} b_i^TS_{:,i} + \beta(K_{ii} - 2K_{:,i}S_{:,i} + S_{:,i}^TKS_{:,i}) \quad s.t. 1^Ts_i = 1, s_{ij} > 0 \tag{23}$$

where $b_{ij} = \alpha||y_{i,:} - y_{j,:}||_2^2 + \gamma||f_{i,:} - f_{j,:}||_2^2$. Further, (23) is equivalent to:

$$\min_{S_{:,i}} \beta S_{:,i}^T K S_{:,i} + (b_i^T - 2\beta K_{:,i}) S_{:,i} \quad s.t. 1^T s_i = 1, s_{ij} > 0 \tag{24}$$

Equation (24) is a quadratic programming problem, which can be solved by the related algorithm in Kang et al. (2017) or MATLAB toolkit.

3.6. Complexity Analysis

Algorithm 1 MLCGL

Input: multi-view data $\{X^1, \cdots, X^V\}$, the dimension d of latent representation Y, the cluster number c, and the hyper-parameters α, β, γ.
Initialize: Initialize $S, W = 0$, and Y is a matrix with random values.
While not convergence, **do**:
1: update F according to (13).
2: update W according to (16).
3: update Y according to (20).
4: For each column vector of S, update according to (24).
End
Output: S, W, Y, F.

The whole iteration process of MLCGL is shown in Algorithm 1. In every single iteration, the complexity of update F is $O(cn^2)$, the complexity of update W is $O(d^2 \sum d_v + (\sum d_v)^3)$. The complexity of solving the Sylvester equation when updating Y is $O(d^3)$. The complexity of quadratic programming is $O(n^3)$, so updating S requires $O(n^4)$. Because of $d \ll \sum d_v, c \ll n$, the total complexity of a single iteration is about $O(n^4 + (\sum d_v)^3)$. The complexity to initialize S is $O(Vnc\hat{d}), \hat{d} = \max(d_1, , d_v)$. Suppose total iterations is t, the total complexity is about $O(tn^4 + t(\sum d_v)^3 + Vnc\hat{d})$.

4. Experiment

In this section, we evaluate the performance of MLCGL on five real-world datasets. And Table 1 describes the details of the datasets. We compare the proposed MLCGL with the multiple state-of-art algorithms. And we use five evaluation metrics: F-score, Precision, Recall, NMI (normalized mutual information), and ARI (adjusted rand index) to measure the clustering performance.

4.1. Datasets Description

MSRC-v1 Winn and Jojic (2005): A picture dataset, which contains 210 samples in 7 categories such as trees, buildings, and airplanes. In our experiment, four views are used, which are CM feature, GIST feature, LBP feature, and GENT feature.

Table 1: Dataset Describe

Dataset	Numbers	c	d_1	d_2	d_3	d_4
MSRC-v1	210	7	24	512	256	254
Caltech101-5	240	5	782	144	213	
3Sources	169	6	3560	3631	3068	
Prokaryotic	551	4	438	3	393	
WebKB	203	4	1703	230	230	

Caltech101-5[1]: A picture dataset, which contains 101 types of objects such as faces, animals, and landscapes. This experiment uses a subset of the original dataset, which contains 240 samples in 5 categories. The used views are Gray feature, HOG feature, and LBP feature.

3Sources[2]: A news articles dataset collected from three online sources: BBC, Reuters, and The Guardian. This experiment used 169 news of the original 948 articles. All articles are in the bag-of words representation.

ProkaryoticBrbić et al. (2016): This data set contains 551 samples in 4 categories. All samples are described as heterogeneous, including data and different genomic representations. Three views used in this experiment are textual description, proteome composition, and an indicator denoting the presence/absence of gene families in a genome.

WebKB[3]: This dataset contains 203 web pages in 4 categories. Each web-page is described by the content of the page, the anchor text of the hyper-link, and the text in its title.

4.2. Compare Method

Co-Regularized Spectral Clustering (**Co-reg**)Kumar et al. (2011): It assumed the cluster membership among views are consistent, and co-regularizes the membership to obtain the common clustering indicator.

Robust Multi-View Spectral Clustering (**RMSC**)Xia et al. (2014): This algorithm introduces the standard Markov chain to clustering.

Multi-View Clustering with Adaptive Neighbors (**MLAN**)Nie et al. (2017): Adaptively learn view weights and dynamically learn the local structure of the data.

Latent Multi-view Subspace Clustering (**LMSC**)Zhang et al. (2018): Assume that multi-view data are all mapped from the shared latent representation.

Multi-view Low-Rank Sparse Subspace Clustering (**MLRSC**)Brbić and Kopriva (2018): Learn the global structure via self-representation on each view, and weigh the discrepancy of different views through a regularization term.

Weighted Multi-View Spectral Clustering (**WMSC**)Zong et al. (2018): Dynamically learn the weights of different views through the spectral perturbation theory. And according to the view's weight, the clustering results of spectral clustering tends to be consistently on different views.

1. http://www.vision.caltech.edu/Image$_{D}atasets/Caltech$101/
2. http://mlg.ucd.ie/datasets/3sources.html
3. https://linqs.soe.ucsc.edu/data

Graph-based Multi-View Clustering (**GMC**)Wang et al. (2019): Dynamically learn the local structure and the view weight of different views, then integrate the local structure into a shared similarity graph according to the weight.

4.3. Clustering Results Comparison

Table 2 to Table 6 show the clustering comparison performance respectively yielded by eight different methods on five datasets. For each metric, higher values indicate better performance. And the best result values are **bold**.

From the clustering experiment results in Table 2 to Table 6, it can be seen that comparing the multiple algorithms proposed recently, MLCGL can always achieve excellent performance on different datasets. Specifically, on the MSRC-v1 and Caltech101-5 datasets, MLCGL achieves the best performance in all clustering performance metrics. In particular, on MSRC-v1, MCLGL's performance improvements over the second-best method more than 5%, while on Caltech101-5, the increasement has reached about 10%. On 3 Sources and Prokaryotic, only the recall of MCLGL failed to achieve the optimal performance, while the remaining performance metrics all greatly exceed the comparison algorithms. On WebKB, MCLGL achieves the optimal performance in the three clustering performance indicators, while the other two metrics are close to the best.

Table 2: MSRC-v1

Method	**F-score**	**Precision**	**Recall**	**NMI**	**ARI**
Co-reg	0.481±0.033	0.453±0.037	0.514±0.033	0.515±0.031	0.392±0.040
RMSC	0.674±0.033	0.656±0.035	0.693±0.031	0.705±0.026	0.705±0.039
MLAN	0.698±0.001	0.638±0.001	0.771±0.001	0.752±0.001	0.644±0.001
LMSC	0.739±0.022	0.730±0.031	0.748±0.025	0.765±0.030	0.696±0.041
MLRSSC	0.528±0.026	0.518±0.027	0.537±0.017	0.566±0.014	0.450±0.026
WMSC	0.663±0.014	0.640±0.034	0.687±0.011	0.693±0.012	0.606±0.013
GMC	0.675±0	0.612±0	0.753±0	0.714±0	0.616±0
MLCGL	**0.806±0.005**	**0.792±0.005**	**0.820±0.006**	**0.820±0.006**	**0.774±0.006**

Table 3: Caltech101-5

Method	**F-score**	**Precision**	**Recall**	**NMI**	**ARI**
Co-reg	0.630±0.013	0.615±0.017	0.647±0.010	0.618±0.013	0.535±0.017
RMSC	0.681±0.011	0.646±0.008	0.718±0.021	0.702±0.012	0.596±0.011
MLAN	0.609±0	0.521±0	0.732±0	0.617±0	0.490±0
LMSC	0.745±0.002	0.748±0.002	0.742±0.002	0.736±0.004	0.682±0.002
MLRSSC	0.718±0.006	0.657±0.019	0.794±0.013	0.744±0.007	0.640±0.009
WMSC	0.662±0.013	0.638±0.011	0.687±0.021	0.691±0.011	0.574±0.010
GMC	0.688±0	0.619±0	0.776±0	0.718±0	0.599±0
MLCGL	**0.851±0.012**	**0.847±0.013**	**0.855±0.010**	**0.832±0.012**	**0.813±0.015**

Table 4: 3Sources

Method	F-score	Precision	Recall	NMI	ARI
Co-reg	0.490±0.041	0.534±0.064	0.454±0.032	0.518±0.038	0.351±0.057
RMSC	0.393±0.011	0.417±0.022	0.372±0.017	0.465±0.009	0.223±0.025
MLAN	0.683±0	0.609±0	0.777±0	0.689±0	0.571±0
LMSC	0.410±0.003	0.494±0.002	0.350±0.003	0.387±0.005	0.269±0.003
MLRSSC	0.572±0.024	0.656±0.030	0.508±0.028	0.620±0.017	0.463±0.029
WMSC	0.430±0.016	0.424±0.014	0.435±0.020	0.471±0.015	0.254±0.017
GMC	0.605±0	0.484±0	**0.805±0**	0.621±0	0.443±0
MLCGL	**0.771±0.019**	**0.767±0.049**	0.778±0.030	**0.747±0.008**	**0.700±0.028**

Table 5: Prokaryotic

Method	F-score	Precision	Recall	NMI	ARI
Co-reg	0.452±0.007	0.552±0.009	0.383±0.007	0.284±0.013	0.191±0.011
RMSC	0.562±0.019	0.660±0.011	0.489±0.016	0.394±0.021	0.341±0.020
MLAN	0.577±0.005	0.444±0.009	**0.827±0.008**	0.239±0.010	0.132±0.006
LMSC	0.605±0.022	0.673±0.027	0.533±0.031	0.434±0.017	0.389±0.033
MLRSSC	0.591±0.056	0.725±0.068	0.499±0.048	0.437±0.039	0.389±0.082
WMSC	0.500±0.031	0.585±0.027	0.436±0.019	0.388±0.030	0.245±0.011
GMC	0.461±0	0.447±0	0.476±0	0.193±0	0.091±0
MLCGL	**0.671±0.020**	**0.757±0.022**	0.603±0.013	**0.487±0.015**	**0.494±0.035**

Table 6: WebKb

Method	F-score	Precision	Recall	NMI	ARI
Co-reg	0.604±0.056	0.640±0.040	0.579±0.087	0.343±0.034	0.373±0.072
RMSC	0.591±0.014	0.607±0.017	0.576±0.010	0.281±0.012	0.338±0.025
MLAN	0.668±0	0.559±0	0.831±0	0.402±0	0.373±0
LMSC	0.683±0.006	**0.729±0.006**	0.641±0.006	0.473±0.007	0.497±0.010
MLRSSC	0.714±0.028	0.648±0.046	0.792±0.037	0.468±0.056	0.490±0.064
WMSC	0.474±0.014	0.574±0.011	0.403±0.017	0.287±0.015	0.221±0.013
GMC	0.688±0	0.582±0	**0.840±0**	0.413±0	0.417±0
MLCGL	**0.723±0.014**	0.670±0.005	0.790±0.052	**0.513±0.011**	**0.518±0.031**

4.4. Parameter Analysis

Table 7 shows the optimal parameters of MLCGL on each dataset.Fig. 1 presents the relationship between the dimension of the latent representation Y and the clustering performance metric NMI. From the experimental results of the above datasets, the dimensionality of the latent representation has a great influence on the algorithm clustering performance.

Compared with the high dimensionality of the original space, the dimensionality of the latent representation is basically between 10 and 50, which indicated that the original dimensionality may contain too many redundancy and possible noise. After learned the latent representation, the dimensionality of the multi-view data is significantly reduced and the noise is effectively suppressed.

Table 7: Best parameters of each datasets

Dataset	d	α	β	γ
MSRC-v1	50	0.5	0.5	10
Caltech101-5	40	1	0.5	10
3Sources	20	10	0.01	0.5
Prokaryotic	10	0.005	0.005	10
WebKB	10	0.01	1	10

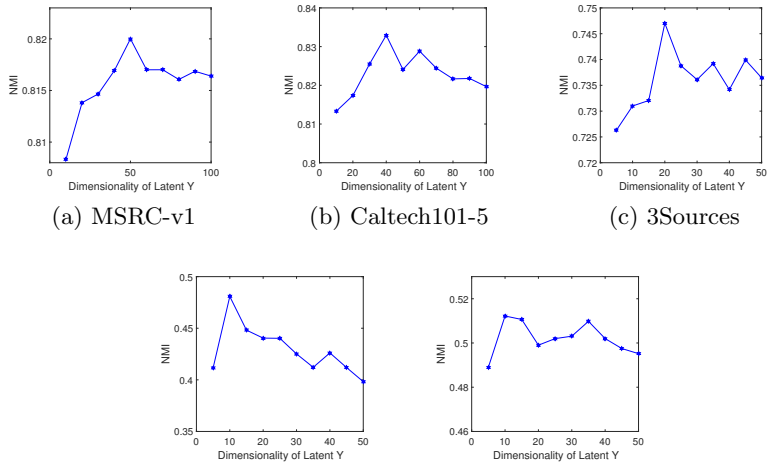

(a) MSRC-v1 (b) Caltech101-5 (c) 3Sources

(d) Prokaryotic (e) WebKB

Figure 1: Dimensionality of latent Y vs NMI.

Figure. 2 shows the relationship among hyper-parameters α, β, and clustering metric NMI, where α affects the preservation of the local structure, and β affects the preservation of the global structure. From the experiments on different datasets, we can see that on Caltech101-5 and 3Sources datasets, the clustering performance is greatly affected by the local structure. For WebKB, the performance is greatly affected by the global structure, and for MSRC-v1 and Prokaryotic, the global structures and local structures have similar influence on clustering performance.

Figure. 3 gives the relationship between the hyper-parameter γ and the clustering performance metric NMI, where γ denotes the influence of the rank constraint introduced on the Laplacian graph on MLCGL. From the experimental results shown in Fig. 3, in the existing parameter range, different hyper-parameters γ have little effect on the clustering

performance. Then, if we extend the parameter search range, another hyper-parameter γ may be searched to obtain better clustering performance.

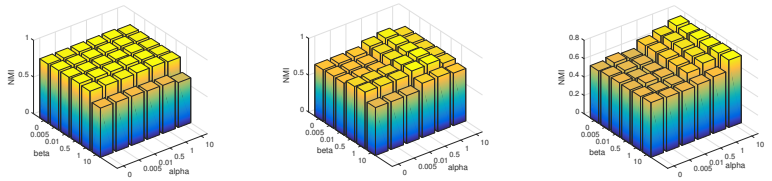

(a) MSRC-v1 (b) Caltech101-5 (c) 3Sources

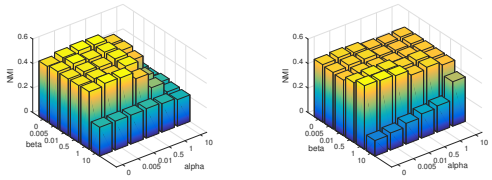

(d) Prokaryotic (e) WebKB

Figure 2: Hyper-parameter α and β vs NMI.

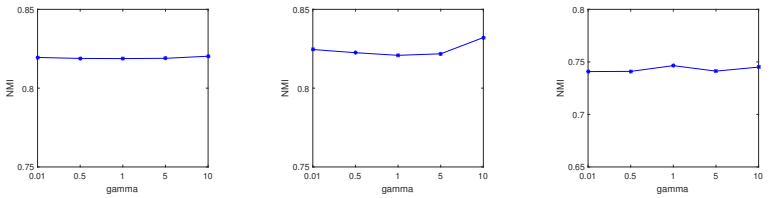

(a) MSRC-v1 (b) Caltech101-5 (c) 3Sources

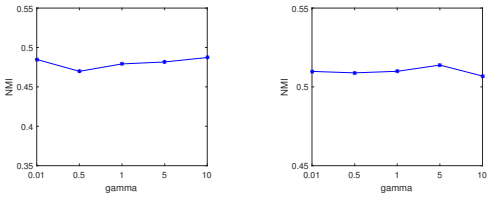

(d) Prokaryotic (e) WebKB

Figure 3: Hyper-parameter γ vs NMI.

4.5. Similarity Graph Comparison

In Fig. 4, MLAN trends to learn the local structure in the original space, LMSC learns the global structure in the latent space, and MLRSSC learns the global structure in the original space. Observing the similarity graph in Fig. 4, the diagonal blocks of MLCGL are denser than others, indicating that our method MLCGL encourages us to lean a denser and distinct diagonal blocks with c connected components.

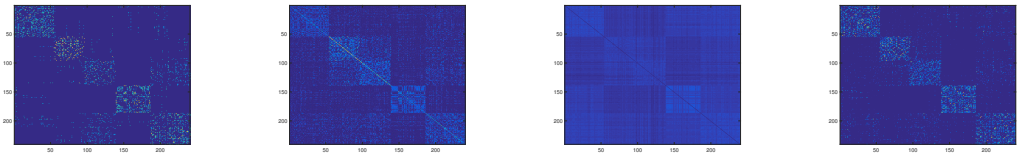

(a) MLAN (b) LMSC (c) MLRSSC (d) Ours

Figure 4: Similarity graph of compare method on Caltech101-5.

4.6. Convergence Analysis

Figure. 5 shows the convergence curves of the objective function in different datasets. Obviously, MLCGL can quickly converge within the first 10 iterations.

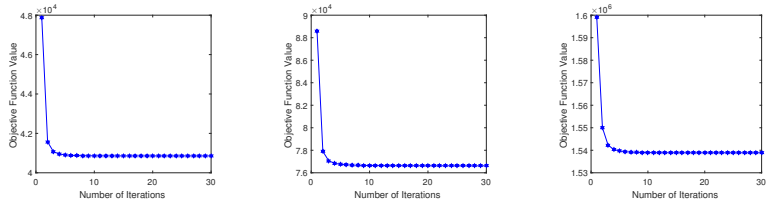

(a) MSRC-v1 (b) Caltech101-5 (c) 3Sources

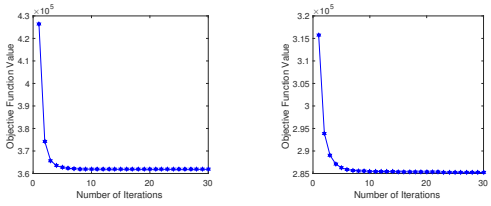

(d) Prokaryotic (e) WebKB

Figure 5: Convergence curve of each datasets.

From the experimental results shown above, it's concluded that MLCGL can learn the local structure and global structure on the latent representation simultaneously. By introducing the rank constraint in the Laplacian graph, MLCGL can further make the clustering performance obtained on the latent representations more reasonable. The convergence curve also presents the efficiency of the algorithm solution.

5. Conclusion

In this paper, we proposed an algorithm named Multi-view Latent subspace Clustering based on both Global and Local structure. MLCGL learns latent representation, similarity graph, and cluster indicator simultaneously in a single model. Experimental results on multiple real-world datasets also prove the excellent performance of MLCGL. But for large-scale datasets, we do not have an effective solution. In the following work, we will try to obtain a robust low-dimensional representation in the framework of Contrastive Learning.

References

Maria Brbić and Ivica Kopriva. Multi-view low-rank sparse subspace clustering. *Pattern Recognition*, 73:247–258, 2018.

Maria Brbić, Matija Piškorec, Vedrana Vidulin, Anita Kriško, Tomislav Šmuc, and Fran Supek. The landscape of microbial phenotypic traits and associated genes. *Nucleic acids research*, page gkw964, 2016.

Man-Sheng Chen, Ling Huang, Chang-Dong Wang, and Dong Huang. Multi-view clustering in latent embedding space. In *AAAI*, volume 34, pages 3513–3520, 2020.

Ky Fan. On a theorem of weyl concerning eigenvalues of linear transformations i. *PNAS*, 35(11):652, 1949.

Han Hu, Zhouchen Lin, Jianjiang Feng, and Jie Zhou. Smooth representation clustering. In *CVPR*, pages 3834–3841, 2014.

Jin Huang, Feiping Nie, and Heng Huang. A new simplex sparse learning model to measure data similarity for clustering. In *IJACI*, 2015.

Shudong Huang, Zhao Kang, Ivor W Tsang, and Zenglin Xu. Auto-weighted multi-view clustering via kernelized graph learning. *Pattern Recognition*, 88:174–184, 2019a.

Zhenyu Huang, Joey Tianyi Zhou, Xi Peng, Changqing Zhang, Hongyuan Zhu, and Jiancheng Lv. Multi-view spectral clustering network. In *IJCAI*, pages 2563–2569, 2019b.

Zhenyu Huang, Peng Hu, Joey Tianyi Zhou, Jiancheng Lv, and Xi Peng. Partially view-aligned clustering. *NeurIPS*, 33, 2020.

Zhao Kang, Chong Peng, and Qiang Cheng. Twin learning for similarity and clustering: A unified kernel approach. In *AAAI*, volume 31, 2017.

Zhao Kang, Guoxin Shi, Shudong Huang, Wenyu Chen, Xiaorong Pu, Joey Tianyi Zhou, and Zenglin Xu. Multi-graph fusion for multi-view spectral clustering. *Knowledge-Based Systems*, 189:105102, 2020.

Abhishek Kumar, Piyush Rai, and Hal Daume. Co-regularized multi-view spectral clustering. *NeurIPS*, 24:1413–1421, 2011.

Yijie Lin, Yuanbiao Gou, Zitao Liu, Boyun Li, Jiancheng Lv, and Xi Peng. Completer: Incomplete multi-view clustering via contrastive prediction. In *Proceedings of the IEEE/CVF Conference on Computer Vision and Pattern Recognition*, pages 11174–11183, 2021.

Xinwang Liu, Lei Wang, Jian Zhang, Jianping Yin, and Huan Liu. Global and local structure preservation for feature selection. *IEEE Transactions on Neural Networks and Learning Systems*, 25(6):1083–1095, 2013.

Bojan Mohar, Y Alavi, G Chartrand, and OR Oellermann. The laplacian spectrum of graphs. *Graph theory, combinatorics, and applications*, 2(871-898):12, 1991.

Feiping Nie, Jing Li, Xuelong Li, et al. Parameter-free auto-weighted multiple graph learning: a framework for multiview clustering and semi-supervised classification. In *IJCAI*, pages 1881–1887, 2016.

Feiping Nie, Guohao Cai, and Xuelong Li. Multi-view clustering and semi-supervised classification with adaptive neighbours. In *AAAI*, volume 31, 2017.

Feiping Nie, Lai Tian, and Xuelong Li. Multiview clustering via adaptively weighted procrustes. In *ACM SIGKDD*, pages 2022–2030, 2018.

Hong Peng and Hongmin Cai. Multi-view clustering through self-weighted high-order similarity fusion. In *ICME*, pages 1–6. IEEE, 2021.

Zhenwen Ren and Quansen Sun. Simultaneous global and local graph structure preserving for multiple kernel clustering. *IEEE transactions on neural networks and learning systems*, 2020.

Grace Wahba. A least squares estimate of satellite attitude. *SIAM review*, 7(3):409–409, 1965.

Beilei Wang, Yun Xiao, Zhihui Li, Xuanhong Wang, Xiaojiang Chen, and Dingyi Fang. Robust self-weighted multi-view projection clustering. In *AAAI*, volume 34, pages 6110–6117, 2020.

Hao Wang, Yan Yang, and Bing Liu. Gmc: Graph-based multi-view clustering. *IEEE Transactions on Knowledge and Data Engineering*, 32(6):1116–1129, 2019.

Martha White, Yaoliang Yu, Xinhua Zhang, and Dale Schuurmans. Convex multi-view subspace learning. In *NeurIPS*, pages 1682–1690. Lake Tahoe, Nevada, 2012.

John Winn and Nebojsa Jojic. Locus: Learning object classes with unsupervised segmentation. In *ICCV*, volume 1, pages 756–763. IEEE, 2005.

Rongkai Xia, Yan Pan, Lei Du, and Jian Yin. Robust multi-view spectral clustering via low-rank and sparse decomposition. In *AAAI*, volume 28, 2014.

Changqing Zhang, Huazhu Fu, Qinghua Hu, Xiaochun Cao, Yuan Xie, Dacheng Tao, and Dong Xu. Generalized latent multi-view subspace clustering. *IEEE transactions on pattern analysis and machine intelligence*, 42(1):86–99, 2018.

Linlin Zong, Xianchao Zhang, Xinyue Liu, and Hong Yu. Weighted multi-view spectral clustering based on spectral perturbation. In *AAAI*, volume 32, 2018.